# Claudin-1 as a novel target gene induced in obesity and associated to inflammation, fibrosis and cell differentiation.

Pablo Fernández-García[1]*, Siri D. Taxerås[2]*, Marjorie Reyes-Farias[2,3], Lorena González[2], Andrea Soria-Gondek[4], Silvia Pellitero[5,6], Jordi Tarascó[7], Pau Moreno[7], Lauro Sumoy[2], Jacqueline M. Stephens[8], Lindsey G. Yoo[8], María Galán[1], Adriana Izquierdo[1], Gema Medina-Gómez[1], Laura Herrero[3,9], Patricia Corrales[1], Francesc Villarroya[9,10], Rubén Cereijo[9,10,11#], David Sánchez-Infantes[1,2,9#]

[1] Department of Basic Health Sciences, Campus Alcorcón, University Rey Juan Carlos (URJC), E-28922 Madrid, Spain.

[2] Fundació Institut Germans Trias i Pujol, Barcelona, 08916, Spain.

[3] Department of Biochemistry and Physiology, School of Pharmacy and Food Sciences, Institut de Biomedicina de la Universitat de Barcelona (IBUB), Universitat de Barcelona, Barcelona, Spain.

[4] Pediatric Surgery Department, Hospital Universitari Germans Trias i Pujol, Badalona, 08916, Spain.

[5] Endocrinology Department, Hospital Universitari Germans Trias i Pujol, Badalona, 08916, Spain.

[6] Centro de Investigación Biomédica en Red de Diabetes y Enfermedades Metabólicas (CIBERDEM), Madrid, 28029, Spain.

[7] General Surgery Department, Hospital Universitari Germans Trias i Pujol, Badalona, 08916, Spain.

[8]Pennington Biomedical Research Center (PBRC) and Louisiana State University. Baton Rouge Louisiana, USA. 70808

[9] Centro de Investigación Biomédica en Red de Fisiopatología de la Obesidad y Nutrición (CIBEROBN), Instituto de Salud Carlos III, Madrid, 28029, Spain.

[10] Department of Biochemistry and Molecular Biomedicine, and Institute of Biomedicine, University of Barcelona, Barcelona, Spain.

[11] Institut de Recerca Hospital de la Santa Creu i Sant Pau, Barcelona, 08041, Spain.

*Both authors contributed equally to this work

[#]Co-corresponding

**Keywords:** Obesity; immunometabolism; claudin; lymphocytes

**Running title**: Claudin-1 is induced in visceral adipose depot in obesity.

**Word count:** 3624

**Contact info:** Department of Health Sciences, Campus Alcorcón, University Rey Juan Carlos (URJC), E-28922 Madrid, Spain. Electronic address: david.sanchezi@urjc.es

Department of Biochemistry and Molecular Biomedicine, and Institute of Biomedicine, University of Barcelona, Barcelona, Spain. Electronic address: rcereijo@ub.edu

## Abstract

*Objective*

T-lymphocytes from visceral and subcutaneous white adipose tissue (vWAT and sWAT, respectively) can have opposing roles in the systemic metabolic changes associated with obesity. However, few studies have focused on this subject. Claudin-1 (*CLDN1*) is a protein involved canonically in Tight Junctions (TJs) and tissue paracellular permeability.

We evaluated T lymphocytes gene expression in vWAT and sWAT and in the whole adipose depots in human samples.

*Methods*

A Clariom D-based transcriptomics analysis was performed on T lymphocytes magnetically separated from vWAT and sWAT from patients with obesity (Cohort 1; N = 11). Expression of candidate genes resulting from that analysis was determined in whole WAT from individuals with and without obesity (Cohort 2; Patients with obesity: N = 13; Patients without obesity: N=14).

*Results*

We observed transcriptional differences between T lymphocytes from sWAT compared to vWAT. Specifically, *CLDN1* expression was found to be dramatically induced in vWAT T cells relative to those isolated from sWAT in patients with obesity. *CLDN1* was also induced in obesity in vWAT and its expression correlates with genes involved in inflammation, fibrosis and adipogenesis.

*Conclusion*

These results suggest *CLDN1* is a novel marker induced in obesity, and differentially expressed in T lymphocytes infiltrated in human vWAT as compared to sWAT. This protein may have a crucial role in the crosstalk between T lymphocytes and other adipose tissue cells and may contribute to inflammation, fibrosis and alter homeostasis and promote metabolic disease in obesity.

**Abbreviations:**

Visceral white adipose tissue (vWAT), subcutaneous white adipose tissue (sWAT), white adipose tissue (WAT), tight junction (TJ), Claudin-1 (CLDN1 for protein; *CLDN1* for gene), body mass index (BMI), Homeostatic model assessment – insulin resistance (HOMA-IR), fetal bovine serum (FBS), phosphate saline buffer (PBS), magnetic-activated cell sorting (MACS), bovine serum albumin (BSA), 4',6-diamidino-2-phenylindole (DAPI)

**Significance Statement:**

Several studies have shown a direct involvement of Claudin-1 in the development and progression of multiple cancers. However, to our knowledge, little information about the role of Claudin-1 in adipose tissue and obesity has been reported yet. Furthermore, Claudin-1 has recently been identified as a therapeutic target for tissue fibrosis in different types of organs, including liver, lung and kidney. In this paper, a novel transcriptomic of human sWAT and vWAT T lymphocytes has been developed. *CLDN1* comes up as a gene strongly regulated in a depot-dependent manner and correlates with genes involved in inflammation and fibrosis. Our results postulate claudin-1 as a novel target in lipotoxicity, obesity and metabolism.

## 1. Introduction

Obesity is defined as an excessive accumulation of lipids in white adipose tissue (WAT) as a result of prolonged positive energy balance (1–3). WAT is a heterogeneous tissue consisting of mature adipocytes and nonadipocyte cells (4–7). Furthermore, WAT has significant endocrine capabilities mediated by a wide range of adipokines and cytokines and impacting multiple body processes (8–10). In humans, WAT has been considered the largest endocrine tissue classified in two main depots, visceral and subcutaneous WAT (vWAT and sWAT, respectively), with morphologic and metabolic differences (11,12). In obesity, WAT expands, leading to dysfunctions characterized by immune cell infiltration (13,14). T lymphocytes ($CD3^+$) play a central role in immune responses and constitute one of the main immune cells infiltrating adipose depots (14). However, few studies in obese humans have focused on T-cell infiltration in WAT and its association with inflammation and metabolic disturbances (15–18).

Here, we show for the first time a transcriptomic analysis of human vWAT- and sWAT-infiltrated T lymphocytes and identify *CLDN1* as a key factor distinctly up-regulated specifically in vWAT-infiltrated T-cells compared to those from sWAT in patients with obesity.

## 2. Methods

The study was approved by the Ethical Committee of the Hospital Germans Trias i Pujol (Badalona, Spain) and follows the guidelines of Helsinki convention. Participants gave their written informed consent before clinical data collection.

### *2.1 Study Participants*

Two different cohorts of patients were enrolled (Table 1, Supplemental Figure S1). All patients were evaluated by the same endocrinologist (S.P.) following the institutional protocol for bariatric surgery (BS) between October 2015 and September 2021, according to BS criteria

(Spanish Position Statement between Obesity, Endocrinology, Diabetes and Surgery Societies). Since cohort 1 was made up only of patients with obesity, a cohort 2 made up of patients with and without obesity was included. The primary reason to use cohort 2 was to have a normal-weight control group to check the levels of *CLDN1* gene expression in these individuals to compare them with obesity condition. The limitation of that was to use total WAT instead of adipose tissue lymphocytes, but there were no options to isolate T cells from healthy donors in our hospital. For Cohort 1, 11 patients with obesity (BMI>35 kg/m$^2$) were enrolled, and vWAT and sWAT from the same patient were collected during BS. For Cohort 2, 27 patients with or without severe obesity (BMI>35 kg/m$^2$ or BMI<27 kg/m$^2$, respectively) were enrolled. For the first group, vWAT and sWAT biopsies were collected when they attended to BS; for the latter on occasion of consultation/minor surgery, mainly cholecystectomy. Exclusion criteria for all cohorts were having cancer, active infectious or inflammatory pathologies other than those related to obesity and treatment with immunosuppressant drugs or suffering from other forms of immunosuppression.

*2.2 Human serological analysis*

Serum samples were collected after 12 h fasting and frozen at –20º C. In the case of cohort 2, serum samples from patients with obesity were obtained at baseline (during the surgery) and 6 months after the surgery. Glucose and insulin levels, as well as lipid profiles (total cholesterol, HDL and LDL cholesterol, and triglycerides), were measured in the certified core clinical laboratory. The Homeostatic model assessment-insulin resistance (HOMA-IR) score was calculated as: $HOMA-IR=\frac{\left[Glu\cos e\frac{mg}{dL}\right]\times\left[Insulin\frac{m.u.int}{dL}\right]}{405}$.

*2.3 Cohort 1: adipose tissue collection, T-cell extraction and counting.*

vWAT and sWAT samples (n=22 in total) were obtained from the 11 patients from Cohort 1 during BS. Fresh WAT collected during surgeries was transferred into two 50 mL tubes containing a 2% fetal bovine serum (FBS) in phosphate saline buffer (PBS) solution and placed on separate multiwell plate submerged in collagenase and Hank's Balanced Salt Solution (pH=7.1). The tissue was then minced into small pieces followed by several centrifugation and supernatant removal steps as previously published (19). $CD3^+$ cells were then labeled with anti-$CD3^+$ MicroBeads and magnetically separated from unlabeled cells using magnetic-activated cell sorting (MACS) columns (Miltenyi Biotec S.L.). Briefly, cell suspension was centrifuged (300 x g, 10 min) and the supernatant completely discarded. Next, the pellet was resuspended in 82 µL of MACS buffer and 2 µL were diluted with 18 µl MACS buffer and reserved at 4º C to evaluate $CD3^+$ cell percentage. Then, 20 µL of $CD3^+$ MicroBeads were added to 80 µL of cell suspension, mixed and incubated for 15 min in ice. Next, cells were washed by adding 2 mL of MACS buffer and centrifuged (300 x g, 10 min, 4º C). Then the pellet was resuspended in 500 µL MACS buffer and maintained in ice.

Meanwhile, the MidiMACS™ Starting Kit (LS) separation column was prepared by placement in the magnetic field on the MidiMACS™ Separator and rinsed with 3 mL of MACS buffer. Once the column reservoir was empty, the cell suspension was added into the column. When all suspension passed, the column was washed by adding twice 3 mL MACS buffer. Afterwards, the column was removed from the magnetic field, and placed onto a new 15 mL conical tube (collection tube). Then, 5 mL MACS buffer was added and the fraction with the magnetically labeled cells was immediately flushed out applying the plunger supplied with the column. 20 µL of the eluted fraction was reserved in ice. Next, the $CD3^+$ fraction of cells was centrifuged (300 x g, 4 min, 4º C), 4 mL of the supernatant was discarded, and the pellet was resuspended in the remaining volume, transferred into a 1.5 mL conical tube and centrifuged (11000 x g, 5 min). The resulting pellet was used to perform RNA extraction.

The reserved aliquots from vWAT and sWAT were labeled to quantify the viability and the number of infiltrated $CD3^+$ cells, respectively. For this purpose, 10 µL of cell samples were mixed with 48 µL MACS Buffer, 2 µL of 7-AAD and 0.5 µL of $CD3^+$. The mix was incubated in darkness for 10 min and then 10 µL of counting beads were added. Isolated T-cells were detected by flow cytometry (FACSCanto II, BD Biosciences). In this system, the optic consists of an excitation source and a three-laser system: blue (488 nm, air-cooled, 20-mV solid state), red (633 nm, 17-mV HeNe) and violet (405 nm, 30-mV solid state) allowing measurement of 8 parameters (FSC, SSC and 6 fluorescence detectors) with carrousel acquisition option for tubes to separate cells are based on their size and fluorescence. FACSDiva and FlowJo (Tree Star Inc.) were used for quantification analyses, graphical representation and gating strategy. Viability, percent, and concentration (cells/µL) of T-cells ($CD3^+$) in vWAT and sWAT was measured. The concentration (cells/mL) was calculated as:

$$\frac{\#Events\,(viability)}{2500\,beads} \times \frac{1036\,beads}{1\,\mu L} \times \frac{10^3\,\mu L}{1\,mL} = cells/mL.$$

Total RNA was then extracted using an affinity column-based methodology suitable for small amounts of biological material (NucleoSpin RNA XS; Mecherey-Nagel, Duren, Germany). RNA yield and purity were determined by spectrophotometry and RNA integrities were assessed with the Nano 6000 assay on Agilent's 2100 Bioanalyzer.

*2.4 Clariom D Assay*

$CD3^+$ cell extracted RNA was reverse transcribed into cDNA, amplified and biotinylated by *in vitro* transcription (MultiScribe TaqMan Reverse Transcription Reagents; ThermoFisher Scientific, Waltham, MA, USA). Labeled cDNAs were hybridized onto Clariom D Human Assay Microarrays, which include probe sets enabling transcriptome-wide gene- and exon-level expression profiling (Affymetrix, ThermoFisher Scientific). The arrays were washed and scanned using the GeneChip 3000 system (Affymetrix). Transcript Analysis Console (TAC

v4.0; Affymetrix) was used for initial hybridization quality assessment and data inspection. The experimental design for hybridization processing included 4 batches of 9-11 samples each with balancing among different batches between the two compared conditions, vWAT and sWAT.

*2.5 Gene expression analysis*

All statistical analyses of microarray data were performed using R-based software R-4-0-3 environments. Quality control was performed using the array QualityMetrics package. Background correction, probe set summarization and normalization were performed with the oligo package using the most up to date annotation in Bioconductor 3.12. A paired-sample design comparing vWAT and sWAT from the same individuals was applied. Subsequent differential expression analysis using the Limma package at the gene level focusing on known genes (with assigned gene symbols). Transcripts were considered for further analyses if they matched the double criteria or false detection rate (FDR) < 0.05 and log (fold change) vWAT vs sWAT > 1.5. Exploratory inference of putatively affected biological functions was performed using Gorilla, harnessing Gene Ontology categories to perform pathway analyses. In-depth functional enrichment analyses were undertaken with Gene Set Enrichment Analysis (GSEA), with results visualized with the Enrichment Map tool in Cytoscape. Pre ranked based analyses were performed using ranking by log2ratio or signed –log10 p-values on relevant MaSigDB gene set collections (v7.1).

*2.6 Adipose tissue collection and RNA isolation and processing from Cohort 2*

Whole vWAT and sWAT samples were obtained from 27 patients from Cohort 2 (13 with severe obesity and 14 without obesity). In this case, fresh WAT collected during surgeries was transferred into liquid nitrogen and then frozen at -80 ºC; another fragment was cut with a sterile scalpel and reserved for histological analyses.

*2.7 Immunofluorescence staining*

CLDN1 location in AT samples was assessed by immunofluorescence. Briefly, tissue samples were fixed in 4% formaldehyde overnight and included in paraffin. Paraffin blocks were histologically cut (5 μm), 3 nonconsecutive sections per sample were collected on slides and dewaxed. Subsequently, samples were submerged into Tris-EDTA buffer (pH = 7.9), microwaved until boiling 3x and allowed to cool. Afterwards, they were rinsed with 1x PBS-Triton 100 (0.02%) and blocking was conducted using fish gelatin dissolved in PBS-Triton with 2% bovine serum albumin (BSA). Anti-CLDN1 antibody (Abcam®, ab15098; 1:75) was added to the prepared histological cuts and incubated overnight at 4º C in darkness. Samples were then washed with 1x PBS-Triton to remove antibody excess and secondary antibody was added (Jackson Immuno Research®, 111-585-144; 1:250) and incubated at room temperature for 1 h. After, the samples were washed again with 1x PBS-Triton prior to nuclei staining with fluorescent marker 4',6-diamidino 2-phenylindole (DAPI) for 15 minutes. Finally, mounting medium (50% glycerin/PBS-Triton) was added to histological preparations before covering them with coverslips. Samples were stored at 4º C in the darkness until visualization under a FluoView FV300™ confocal microscope (Olympus, Spain). The fluorescence intensity of the signal corresponding to CLDN1 in vWAT and sWAT was quantified using ImageJ.

*2.8 Statistical Analysis of Clinical Features.*

Additional statistical data analysis beyond Bioinformatics procedures was conducted with GraphPad Prism 7.01 (GraphPad Software, Inc., La Jolla, CA, USA) and IBM SPSS 25.0 (IBM, Armond, NY, USA). Assessment of data distribution within groups was analyzed using the Shapiro–Wilk test, while presence of outliers was determined using Tukey's rule (see above). Moreover, the 22 samples included in the study are after outlier removal based on two criteria:

availability of samples from both T-lymphocytes samples derived from both visceral and subcutaneous fat depot from the same individual, passing array quality metrics, hierarchical clustering, and PCA visual inspection. Supplementary figures are included to illustrate the exclusion procedure (Supplemental Figure S2).

If data had a normal distribution, Student's t-test were performed to conduct comparisons between two groups; otherwise, Mann-Whitney's test was used. Likewise, correlations between *CLDN1* and selected genes' expression levels were conducted using the Pearson's (normally distributed) or Spearman's (non-normally) methods. The threshold of statistical significance for all analyses was established at the two-tailed 5% level ($p < 0.05$).

## 3. Results

### *3.1 Clinical parameters*

All patients from Cohort 1 exhibited severe obesity, while Cohort 2 included individuals with severe obesity and controls (Table 1). Specifically, in Cohort 2, the group of patients with severe obesity had a higher weight, BMI, HbA1c%, triglycerides, and lower HDL-cholesterol compared to the control group, thus confirming they exhibited an obesity-associated metabolic disarray beyond an increase in adiposity.

### *3.2 Claudin-1 is a novel target gene modulated in adipose tissue T-cells and in obesity.*

Considering the lack of information about the role of T lymphocytes in terms of gene expression in obesity, we focused on this WAT cell subpopulation. We isolated for the first time enough viable T-cells from vWAT and sWAT in human patients with obesity, and a transcriptomic analysis of this immune cell population was performed.

T lymphocytes isolated by MACS were confirmed as $CD3^+$ by FACS in both vWAT and sWAT, and equal amounts of T cell RNA from both adipose tissues was used to perform an

array (dataset available at GEO repository: GSE236145). It is important to remark that T lymphocytes from sWAT clustered separately of those from vWAT, and also showed different transcriptomic data. Moreover, differential gene expression analyses of T-cell populations in vWAT and sWAT from patients with obesity (Cohort 1) revealed nominally significant differences in genes (FDR pvalue<0.05, absolute fold change >1.5, Figure 1A). Upon multiple testing correction only 13 genes were found to be significant (FDR<0.05 highlighted in red in Figure 1B; Supplemental File S1). Pathway enrichment analysis (Supplemental Figure S3 and Supplemental File S2) revealed a downregulation of pathways related to cellular component organization or biogenesis, developmental process, and extracellular matrix organization in vWAT vs sWAT T lymphocytes. On the other hand, pathways involved in immune response, cell activation and inflammation were upregulated in vWAT compared to sWAT.

*CLDN1* was among the most regulated T-cell genes, showing a dramatic up-regulation in T-cells from vWAT compared to those in sWAT (Figures 1B-C and 2A). Due to the lack of a control group in Cohort 1, *CLDN1* gene expression was measured in Cohort 2 (total sWAT and vWAT from controls and patients with severe obesity). Besides also showing a depot-dependent modulation like in T-cell-based Cohort 1 analyses, whole WAT-based analyses in Cohort 2 revealed higher levels of *CLDN1* mRNA in vWAT from patients with obesity as compared to controls, but not in sWAT (Figure 2B).

### *3.3 CLDN1 is associated with T-cell extracellular matrix remodeling and adipose tissue proinflammatory markers, dyslipidemia, and insulin resistance.*

Transcriptomics regression analyses of T lymphocytes showed positive and negative correlations between expression of *CLDN1* and different genes involved in the extracellular matrix function (Supplemental Table S2). However, *CLDN1* gene expression in total vWAT showed a significant inverse correlation with the expression of genes involved in adipogenesis

and adipose function, such as peroxisome-activated receptor gamma (*PPARG*), fatty acid synthase (*FASN*), hormone-sensitive lipase (*HSL*) and adiponectin (*ADIPOQ*) (Figure 3A). Contrary, *CLDN1* transcript levels correlated positively with genes encoding pro-inflammatory cytokines, including tumor necrosis factor alpha (*TNF*), chemokine (C-X-C) motif ligand 10 (*CXCL10*) and interleukin (IL) 18 (*IL18*), but negatively correlated with other genes encoding known adipose tissue-expressed anti-inflammatory cytokines such as *IL13*, *IL33* and *CXCL14* (Figure 3B). Furthermore, *CLDN1* gene expression in total vWAT showed a significant positive correlation with the expression of genes involved in adipose tissue remodeling by fibrosis, such as collagen type 1 (*COL1A1*), transforming growth factor beta (*TGFβ*), insulin growth factor 1 receptor (*IGF1R*) and inhibitor of nuclear factor kappa B kinase subunit epsilon (*IκBKε*) (Figure 3C).

Moreover, when assessing correlations between *CLDN1* gene expression and clinical parameters in Cohort 2 comparing obesity *vs* control individuals, significant associations were observed with *CLDN1* in vWAT and parameters related to glucose and lipid homeostasis, such as Hb1Ac and triglycerides (directly) and HDL cholesterol (inversely) before BS (time 0) (Table 2). Such associations were no longer statistically significant after 6 months (Table 2).

### *3.4 CLDN1 protein is detectable in WAT from individuals with obesity.*

Finally, we further examined at the protein level whether CLDN1 was distinctly expressed in vWAT and sWAT in obesity. CLDN1 was detected in vWAT and sWAT from 7 obese patients of Cohort 1 indicating that CLDN1 protein detected was notable higher in vWAT than in sWAT, where it was almost nearly undetectable (Figure 4).

## ***4.* Discussion**

Although obesity is characterized by a chronic low-grade inflammation that is typically more extensive in visceral compared to subcutaneous fat (20–22), the gene expression pattern of immune cell types infiltrated in vWAT and sWAT in patients with obesity has not been extensively studied. Our novel transcriptomic data revealed that vWAT T lymphocytes have a different gene profile compared to those located in sWAT. Overall, pathways associated with inflammation were enriched in vWAT T-cells, concordant with the aforementioned previous whole-tissue and other immune cell-focused reports (20,21), whereas metabolic and tissue remodeling-related pathways were repressed. This data could suggest a different cross-talk between T cells and adipocytes occurring in vWAT compared to sWAT, which would lead to a different behavior in terms of gene expression, inflammatory signaling, and adipokines secretion in obesity. Among modulated transcripts, *INTL1* and *CLDN1* were especially upregulated in vWAT-resident T-cells in obesity. Other studies have previously observed depot-dependent modulation of INTL1 (intelectin-1, an adipokine also known as *omentin*) in vWAT (23) while *CLDN1* modulation in obesity has not been fully studied in WAT.

Tight junctions (TJs) require the coordination of different proteins (24). Claudins are a family of transmembrane proteins that play a critical role in TJs function by regulating paracellular barrier permeability, as well as apical cell-cell adhesion (25,26). They confer specificity to permeate across TJs (27). Moreover, they can also participate in tissue fibrosis (27,28).

Claudin-1 (CLDN1) was the first-identified member of the family. It is a 22-kDa protein highly expressed in the intestine, spleen, brain, liver, kidney, and testis (28). CLDN1 has recently been identified as a therapeutic target for tissue fibrosis in some organs (e.g., liver, lung, and kidney) (29). Also, a direct involvement of CLDN1 in the development and progression of multiple cancers has been described (30), but little is known about the presence and possible role of CLDN1 in inflammatory processes in WAT depots, especially in obesity. *CLDN1* is expressed in different cell types, including T-cells (31), but no information about its regulation under

metabolic complications has been reported. Moreover, it has been described that different isoforms of the claudin family promote T-cells migration and infiltration in different tissues by inducing inflammation (32,33).

Our results show that *CLDN1* expression is higher in T lymphocytes from vWAT compared to the sWAT in patients with obesity. Moreover, we show that CLDN1 protein is indeed present in these fat depots, and in higher amount in vWAT than in sWAT. After demonstrating the specificity of *CLDN1* overexpression in vWAT T lymphocytes (Cohort 1), we corroborated this in whole vWAT compared to sWAT from obese individuals (Cohort 2). We observed that the expression of *CLDN1* was also induced in patients with obesity when compared to controls. Our findings are supported by another report where *CLDN1* expression levels were found to be higher in whole vWAT in comparison with sWAT (34).

vWAT is recognized as a depot with a high degree of hypertrophic adipocytes with decreased adipogenesis (35) and high grade of inflammation in obesity (20–22). Moreover, CLDN1 has been associated with fibrosis and cancer progression, and targeting CLDN1 with a monoclonal antibody has been proposed as a potential therapeutic approach in liver models (29). Additionally, to stabilize cell/matrix interactions, the location of CLDN1 in the basal membrane is needed, allowing the regulation of cell/ECM interactions by interacting with integrin molecules via integrin-FAK signaling (36). Given this and the fact that our results also indicated that cell differentiation and extracellular matrix remodeling pathways were downregulated in vWAT T-cells from patients with obesity, we hypothesized that the dramatic up-regulation of *CLDN1* could be due to a dynamic breaking and reannealing in TJ-like strands as a pathological reaction against lipotoxicity. This mechanism to try to balance the homeostasis alteration might cause a leak favoring the transport of inflammatory mediator(s) and effecting the crosstalk between T lymphocytes and the other cells.

Our results show that *CLDN1* gene expression directly correlates with inflammatory genes and inversely with markers of adipogenesis. In addition, *CLDN1* also shows an inverse correlation with the levels of *CXCL14*, a molecule with an anti-inflammation role reported from our laboratories (37). Moreover, a direct correlation between AT fibrosis markers and *CLDN1* gene expression in whole WAT from patients with obesity was found. These results are concomitant with an association of vWAT *CLDN1* levels and metabolic dysregulation in obese individuals, which nonetheless disappear after therapeutic intervention (BS), suggesting a detrimental role of this protein's actions in obesity-associated clinical alterations.

Our study has several limitations: a) the relatively low number of patients in the Cohort 1 ($n$ = 11), lack of enough statistical power to decipher potential age and gender effect, and the lack of T lymphocytes samples from control individuals in this cohort. However, the control individuals from Cohort 2 allowed us to describe the elevated levels of *CLDN1* gene expression in obesity. Moreover, using a publicly available database, a third cohort was analyzed corroborating the data of our study (Supplemental File S3 and S4); b) this data does not distinguish between $CD4^+$ and $CD8^+$ T lymphocytes, and it would be important to check these two subpopulations and their contribution to CLDN1 modulation in vWAT; c) Since patients with obesity use to show higher infiltration of immune cells including T lymphocytes in vWAT, we cannot postulate a conclusion about the final responsibility for increased levels of CLDN1. However, since an equal normalized amount of RNA was used for transcriptomic analyses of both sWAT and vWAT, our results suggest that such higher levels of *CLDN1* are due to a higher gene expression in T cells from vWAT compared to those from sWAT, independently of the amount of these cells.

Nonetheless, a strength of our data is the novel transcriptome analysis of vWAT and sWAT $CD3^+$ T lymphocytes from the same individuals (patients with obesity), allowing specific intraindividual comparisons to analyze the data.

In conclusion, we demonstrate the existence of a distinct gene expression profile of T lymphocytes in vWAT compared to sWAT in humans with obesity, with a marked upregulation of *CLDN1* in the former. Our results suggest that CLDN1 may be involved in the more pathology-inducing adaptation of the vWAT to lipotoxicity. Moreover, our data highlight the importance of performing further research on the role of inter-cellular junctions within adipose depots, in which CLDN1 is likely to be major actor in the context of altered fat plasticity occurring in obesity. Further studies will be necessary to evaluate potential strategies to combat obesity and related metabolic diseases by targeting CLDN1-mediated signaling.

**Funding agencies**

This study was supported by grants CP15/00106, PI17/01455, PI20/00807 from Instituto de Salud Carlos III and the Fondo Europeo de Desarrollo Regional (FEDER) to DS-I., the Spanish Ministry of Science and Innovation (MCIN) (grant PID2020-114953RB-C21 to LH, grant IJC2018-037142-I funded by the MCIN/AEI/10.13039/501100011033 to RC), the Biomedical Research Centre in Pathophysiology of Obesity and Nutrition (CIBEROBN) (Grant CB06/03/0001 to LH), and the Merck Health Foundation (to LH). RC is a Serra Húnter Fellow.

**Disclosure summary**

I certify that neither I nor my co-authors have a conflict of interest as described above that is relevant to the subject matter or materials included in this work.

## References


1. Obesity Update 2017. OECD; https://www.oecd.org/els/health-systems/Obesity-Update-2017.pdf. Updated 2017. Accessed Jan 4, 2023

2. Hill JO, Wyatt HR, Peters JC. Energy Balance and Obesity Energy Balance : Definitions. Circulation. 2012;126(1):126–32.

3. Hill JO, Wyatt HR, Peters JC. Obesity and Weight Management. Eur Endocrinol. 2013;9(2):111–5.

4. Wozniak SE, Gee ÆLL, Wachtel MS, Frezza ÆEE. Adipose Tissue : The New Endocrine Organ ? A Review Article. Dig Dis Sci. 2009;54:1847–56.

5. Coelho M, Oliveira T, Fernandes R. Biochemistry of adipose tissue: an endocrine organ. Archives of Medical Science. 2013;9(2):191–200.

6. Sestan M, Wensveen FM, Valenti S, Turk T. Interactions between adipose tissue and the immune system in health and malnutrition. Semin Immunol. 2015;27:322–33.

7. Kohlgruber AC, Lamarche NM, Lynch L. Adipose tissue at the nexus of systemic and cellular immunometabolism. Semin Immunol [Internet]. 2016;28(5):431–40. Available from: http://dx.doi.org/10.1016/j.smim.2016.09.005

8. Ronti T, Lupattelli G, Mannarino E. The endocrine function of adipose tissue: an update. Clin Endocrinol (Oxf). 2006;64:355–65.

9. Richard AJ, White U, Elks CM, M. Stephens J. Adipose Tissue: Physiology to Metabolic Dysfunction. In: Feingold KR, Anawalt B, Blackman MR, Boyce A, Chrousos G, editors. Endotext. South Dartmouth; 2020.

10. Galic S, Oakhill JS, Steinberg GR. Adipose tissue as an endocrine organ. Mol Cell Endocrinol. 2010;316:129–39.

11. Reyes-Farias M, Fos-domenech J, Serra D, Herrero L, Sánchez-Infantes D. White adipose tissue dysfunction in obesity and aging. Biochem Pharmacol. 2021;192:114723.

12. Kawai T, Autieri M V, Scalia R. Adipose tissue inflammation and metabolic dysfunction in obesity. Am J Physiol Cell Physiol. 2021;320:C375–91.

13. Exley MA, Hand L, Shea DO, Lynch L. Interplay between the immune system and adipose tissue in obesity. Journal of Endocrinology. 2014;223(2):R41–8.

14. Wang Q, Wu H. T Cells in Adipose Tissue : Critical Players in Immunometabolism. Front Immunol. 2018;9:9–11.

15. Lumeng CN, Maillard I, Saltiel AR. T-ing up inflammation in fat. Vol. 15, Nature Medicine. 2009. p. 846–7.

16. Jiang E, Perrard XD, Yang D, Khan IM, Perrard JL, Smith CW, et al. Essential Role of CD11a in CD8+ T-Cell Accumulation and Activation in Adipose Tissue. Arterioscler Thromb Vasc Biol. 2014;34:34–43.

17. Kaminski DA, Randall TD. Adaptive immunity and adipose tissue biology. Trends Immunol [Internet]. 2010;31(10):384–90. Available from: http://dx.doi.org/10.1016/j.it.2010.08.001

18. Otani T, Furuse M. Tight Junction Structure and Function Revisited. Trends Cell Biol [Internet]. 2020;30(10):805–17. Available from: https://doi.org/10.1016/j.tcb.2020.08.004

19. Sanchez-Infantes D, White UA, Elks CM, Morrison RF, Gimble JM, Considine R V., et al. Oncostatin M is produced in adipose tissue and is regulated in conditions of obesity and type 2 diabetes. Journal of Clinical Endocrinology and Metabolism. 2014 Feb;99(2).

20. Salvador J, Silva C, Pujante P, Frühbeck G. Abdominal obesity: An indicator of cardiometabolic risk. Endocrinología y nutrición. 2008;55(9):420–32. Spanish.

21. Zwick RK, Guerrero-juarez CF, Horsley V, Plikus M V. Review Anatomical , Physiological , and Functional Diversity of Adipose Tissue. Cell Metab [Internet]. 2018;27(1):68–83. Available from: https://doi.org/10.1016/j.cmet.2017.12.002

22. Frühbeck G. Adipose Tissue Protocols. Methods in Molecular Biology: Overview of Adipose Tissue and Its Role in Obesity and Metabolic Disorders. 2nd ed. Humana Press; 2008. 1–22 p.

23. Norreen-Thorsen M, Struck EC, Öling S, Zwahlen M, Feilitzen K Von, Odeberg J, et al. A human adipose tissue cell-type transcriptome atlas. Cell Rep. 2022;40(2):111046.

24. Zihni C, Mills C, Matter K, Balda MS. Tight junctions: From simple barriers to multifunctional molecular gates. Nat Rev Mol Cell Biol [Internet]. 2016;17(9):564–80. Available from: http://dx.doi.org/10.1038/nrm.2016.80

25. Cong X, Kong W. Endothelial tight junctions and their regulatory signaling pathways in vascular homeostasis and disease. Cell Signal. 2020;66(November 2019).

26. Günzel D, Yu ASL. Claudins and the modulation of tight junction permeability. Vol. 93, Physiological Reviews. 2013. 525–569 p.

27. Zou J, Li Y, Yu J, Dong L, Husain AN, Shen L, et al. Idiopathic pulmonary fibrosis is associated with tight junction protein alterations. Biochim Biophys Acta Biomembr. 2020 May 1;1862(5).

28. Godfrey RA, Severs NJ, Jeffery K, Jeffery PK. Structural Alterations of Airway Epithelial Tight Junctions in Cystic Fibrosis: Comparison of Transplant and Postmortem TISSue. Vol. 9, Am. J. Respir. Cell Mol. BioI. 1993.

29. Roehlen N, Saviano A, El Saghire H, Crouchet E, Nehme Z, Del Zompo F, et al. A monoclonal antibody targeting nonjunctional claudin-1 inhibits fibrosis in patient-derived models by modulating cell plasticity [Internet]. 2022. Available from: https://www.science.org

30. Bhat AA, Syed N, Therachiyil L, Nisar S, Hashem S, Muralitharan S, et al. Claudin-1 , A Double-Edged Sword in Cancer. Int J Mol Sci. 2020;21:569.

31. Shiozaki A, Bai X hui, Shen-Tu G, Moodley S, Takeshita H, Fung SY, et al. Claudin 1 mediates TNFα-induced gene expression and cell migration in human lung carcinoma cells. PLoS One. 2012 May 31;7(5).

32. Kolchakova D, Moten D, Batsalova T, Dzhambazov B. Tight Junction Protein Claudin-12 Is Involved in Cell Migration during Metastasis. Biomolecules. 2021;11(5):636.

33. Heiskala M, Peterson PA, Yang Y. The Roles of Claudin Superfamily Proteins in Paracellular Transport. Traffic. 2001;2:92–8.

34. Keller M, Hopp L, Liu X, Wohland T, Rohde K, Cancello R, et al. Genome-wide DNA promoter methylation and transcriptome analysis in human adipose tissue unravels novel candidate genes for obesity. Mol Metab [Internet]. 2017;6(1):86–100. Available from: http://dx.doi.org/10.1016/j.molmet.2016.11.003

35. Vishvanath L, Gupta RK. Contribution of adipogenesis to healthy adipose tissue expansion in obesity. J Clin Invest. 2019;129(10):4022–31.

36. Hagen SJ. Non-canonical functions of claudin proteins: Beyond the regulation of cell-cell adhesions. Tissue Barriers [Internet]. 2017;5(2):1–14. Available from: https://doi.org/10.1080/21688370.2017.1327839

37. Cereijo R, Quesada-López T, Gavaldà-Navarro A, Tarascó J, Pellitero S, Reyes M, et al. The chemokine CXCL14 is negatively associated with obesity and concomitant type-2 diabetes in humans. Int J Obes. 2021 Mar 1;45(3):706–10.

## Figure legends

**Figure 1**: **Transcriptomic of T cells infiltrated in white adipose tissue (WAT) from individuals with obesity showed *CLDN1* as a gene modulated in a depot-dependent manner.**

A) Heat map of gene expression comparisons between visceral white adipose tissue (vWAT) and subcutaneous white adipose tissue (sWAT) T-lymphocytes. Legend: red (up-regulated), blue (down-regulated) and white (no modulation)., gene symbol, fold change and fdr significance ("***"=FDR <0.001;"**"=FDR<0.01;"*"=FDR<0.05;"."=FDR<0.1). B) Volcano plot showing significantly- (red) and non-significantly regulated (black) transcripts using limma statistics in Cohort 1 dataset (CLDN1 fold change and FDR values shown in inset box). C) PCA biplot showing overlay of the scorings and loadings, highlighting the genes contributing with most weight into the two PCA components most correlated with adipose tissue depot differences (PC2 and PC5). (red vWAT, green sWAT).

**Figure 2: *CLDN1* is induced in obesity, and its expression levels are higher in T lymphocytes infiltrated in visceral white adipose tissue (vWAT) as compared subcutaneous white adipose tissue (sWAT).**

A) mRNA expression of C*LDN1* in T-cells from vWAT compared to those infiltrated in sWAT in patients with obesity. After normality assessment, a paired data (Wilcoxon) test was used to assess statistically significant ($p<0.05$) differences. The boxplot depicts the median, interquartile range and maximum/minimum values and gray lines indicate intraindividual matching. B) mRNA levels of *CLDN1* in whole adipose tissue from patients with severe obesity compared to controls. A t test was used to assess statistical differences. Error bars indicate means ± SEM. * $p < 0.05$ and ** $p < 0.01$ obesity *vs* control group in vWAT; # $p < 0.05$ vWAT *vs* sWAT.

**Figure 3: *CLDN1* transcript levels are associated with T lymphocytes extracellular matrix remodeling markers, adipose proinflammatory markers, dyslipidemia, insulin resistance and fibrosis markers.**

Spearman's correlations between *CLDN1* mRNA levels and mRNA levels of marker genes in human vWAT involved in: A) Adipogenesis and adipocyte function. B) Inflammatory and anti-inflammatory genes. C) Fibrosis and tissue remodeling marker genes. Spearman's rho and associated *p*-value are indicated in the graphs. Correlations were considered statistically significant for $p<0.05$.

**Figure 4: Claudin-1 (CLDN1) protein is located in WAT from individuals with obesity.**

A) Negative control, DAPI, CLDN1 and Merge (DAPI+CLDN1) confocal fluorescent images of CLDN1 located in visceral white adipose tissue (vWAT) and subcutaneous white adipose tissue (sWAT) from 7 patients with obesity (Cohort 1). Arrows indicate a higher protein expression of CLDN1 in vWAT compared to sWAT. For the 20X magnification the scale bar is 20 µm with a resolution of 4.8272 pixels per micron. For the 60X magnification the scale bar is 10 µm with a resolution of 11.4887 pixels per micron. Original magnification: 60X. Scale bar: 10 µm. B) Graphs showing the quantification of the fluorescence intensity of the vWAT and sWAT localized CLDN1 (****$p < 0.0001$, vWAT vs. sWAT). Three nonconsecutive sections sample (vWAT and sWAT) were used from the same patient.

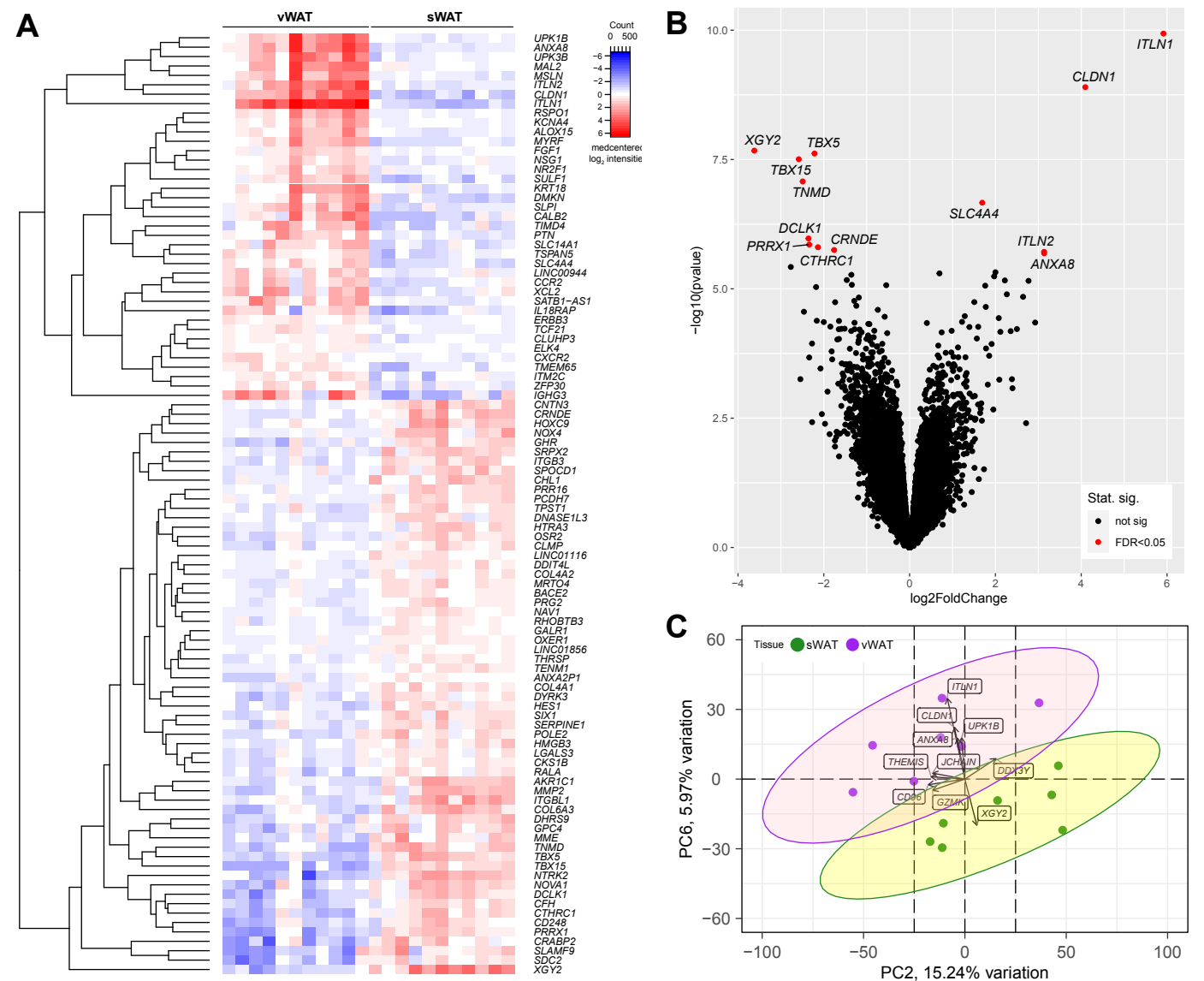
A
vWAT
sWAT
Count
0 500
medcenterec
log2 intensitie
UPK1B
ANXA8
UPK3B
MAL2
MSLN
ITLN2
CLDN1
ITLN1
RSPO1
KCNA4
ALOX15
MYRF
FGF1
NSG1
NR2F1
SULF1
KRT18
DMKN
SLPI
CALB2
TIMD4
PTN
SLC14A1
TSPAN5
SLC4A4
LINC00944
CCR2
XCL2
SATB1−AS1
IL18RAP
ERBB3
TCF21
CLUHP3
ELK4
CXCR2
TMEM65
ITM2C
ZFP30
IGHG3
CNTN3
CRNDE
HOXC9
NOX4
GHR
SRPX2
ITGB3
SPOCD1
CHL1
PRR16
PCDH7
TPST1
DNASE1L3
HTRA3
OSR2
CLMP
LINC01116
DDIT4L
COL4A2
MRTO4
BACE2
PRG2
NAV1
RHOBTB3
GALR1
OXER1
LINC01856
THRSP
TENM1
ANXA2P1
COL4A1
DYRK3
HES1
SIX1
SERPINE1
POLE2
HMGB3
LGALS3
CKS1B
RALA
AKR1C1
MMP2
ITGBL1
COL6A3
DHRS9
GPC4
MME
TNMD
TBX5
TBX15
NTRK2
NOVA1
DCLK1
CFH
CTHRC1
CD248
PRRX1
CRABP2
SLAMF9
SDC2
XGY2
B
ITLN1
CLDN1
XGY2
TBX5
TBX15
TNMD
SLC4A4
DCLK1
PRRX1
CRNDE
CTHRC1
ITLN2
ANXA8
−log10(pvalue)
log2FoldChange
Stat. sig.
not sig
FDR<0.05
C
Tissue
sWAT
vWAT
ITLN1
CLDN1
UPK1B
ANXA8
THEMIS
JCHAIN
DDX3Y
CD96
GZMK
XGY2
PC6, 5.97% variation
PC2, 15.24% variation

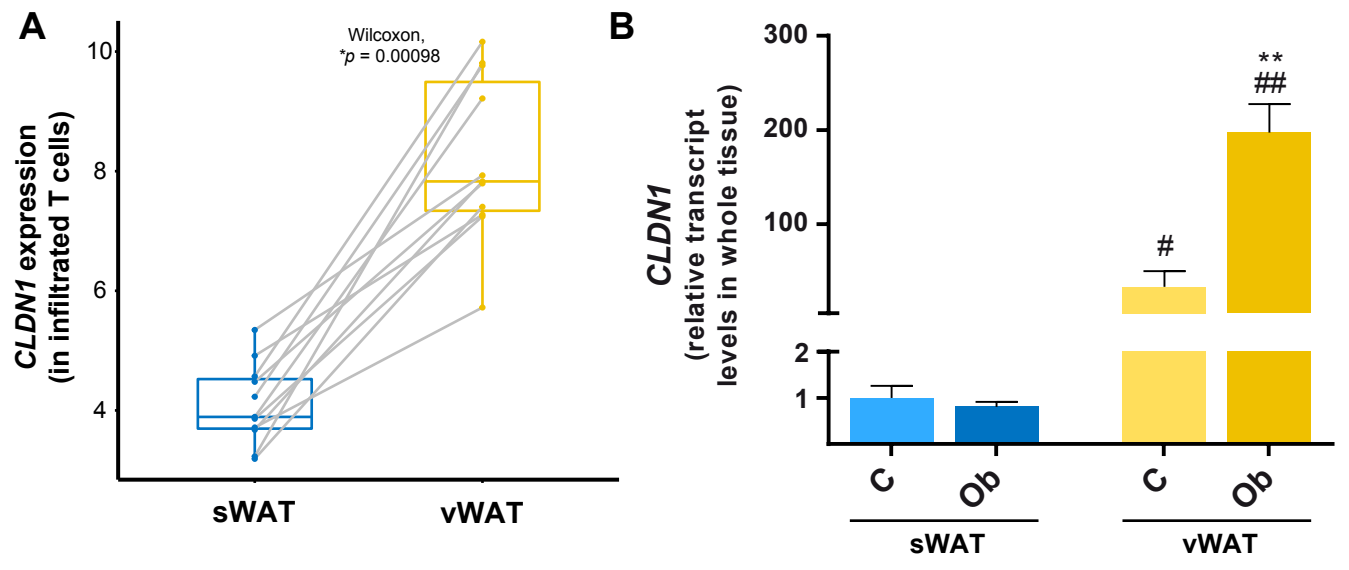
A
Wilcoxon,
*p = 0.00098
CLDN1 expression
(in infiltrated T cells)
10
8
6
4
sWAT
vWAT
B
CLDN1
(relative transcript
levels in whole tissue)
300
200
100
2
1
**
##
#
C
Ob
C
Ob
sWAT
vWAT

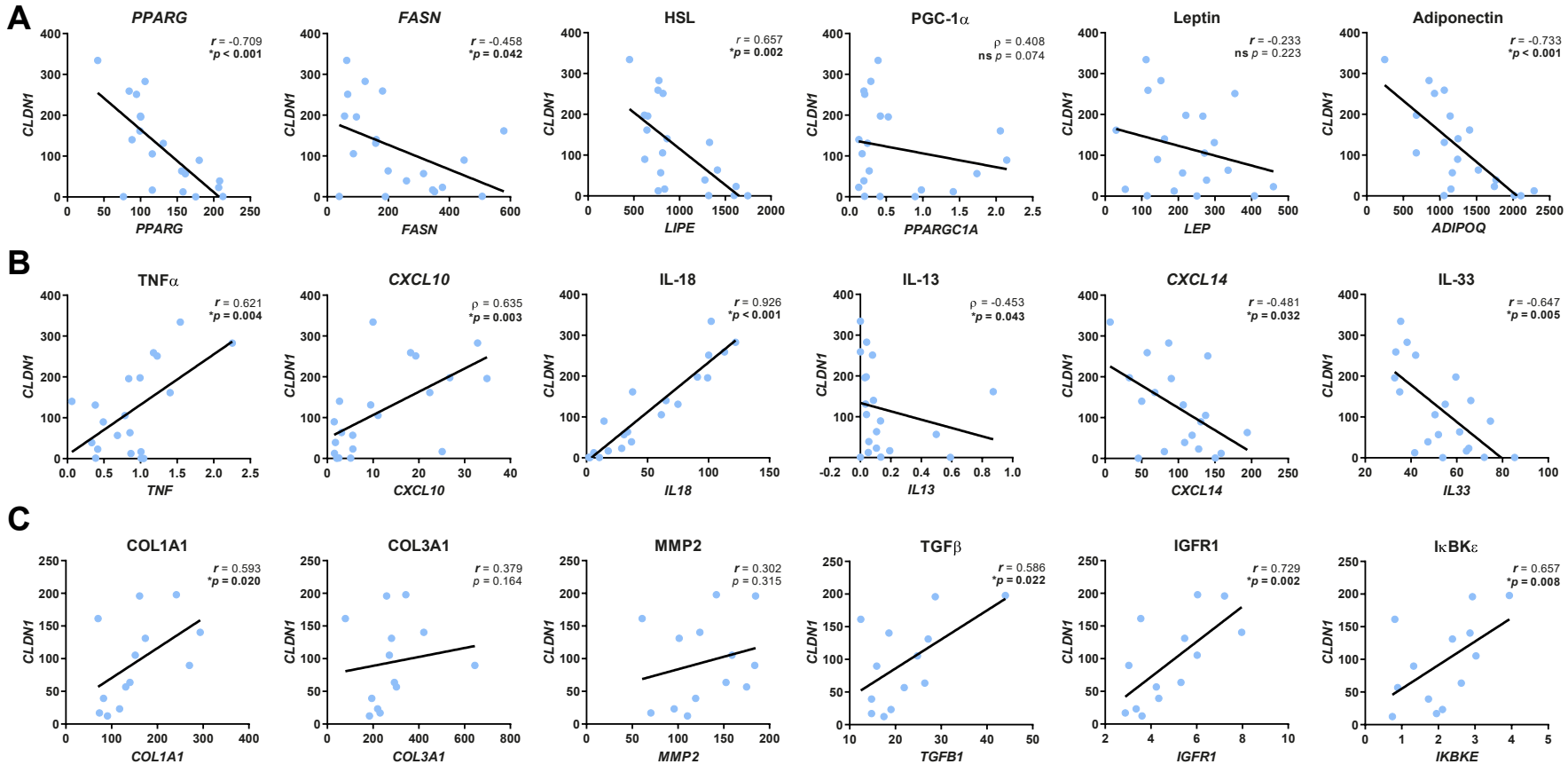
A
PPARG
r = -0.709
*p < 0.001
CLDN1
PPARG
FASN
r = -0.458
*p = 0.042
CLDN1
FASN
HSL
r = 0.657
*p = 0.002
CLDN1
LIPE
PGC-1α
ρ = 0.408
ns p = 0.074
CLDN1
PPARGC1A
Leptin
r = -0.233
ns p = 0.223
CLDN1
LEP
Adiponectin
r = -0.733
*p < 0.001
CLDN1
ADIPOQ
B
TNFα
r = 0.621
*p = 0.004
CLDN1
TNF
CXCL10
ρ = 0.635
*p = 0.003
CLDN1
CXCL10
IL-18
r = 0.926
*p < 0.001
CLDN1
IL18
IL-13
ρ = -0.453
*p = 0.043
CLDN1
IL13
CXCL14
r = -0.481
*p = 0.032
CLDN1
CXCL14
IL-33
r = -0.647
*p = 0.005
CLDN1
IL33
C
COL1A1
r = 0.593
*p = 0.020
CLDN1
COL1A1
COL3A1
r = 0.379
p = 0.164
CLDN1
COL3A1
MMP2
r = 0.302
p = 0.315
CLDN1
MMP2
TGFβ
r = 0.586
*p = 0.022
CLDN1
TGFB1
IGFR1
r = 0.729
*p = 0.002
CLDN1
IGFR1
IκBKε
r = 0.657
*p = 0.008
CLDN1
IKBKE

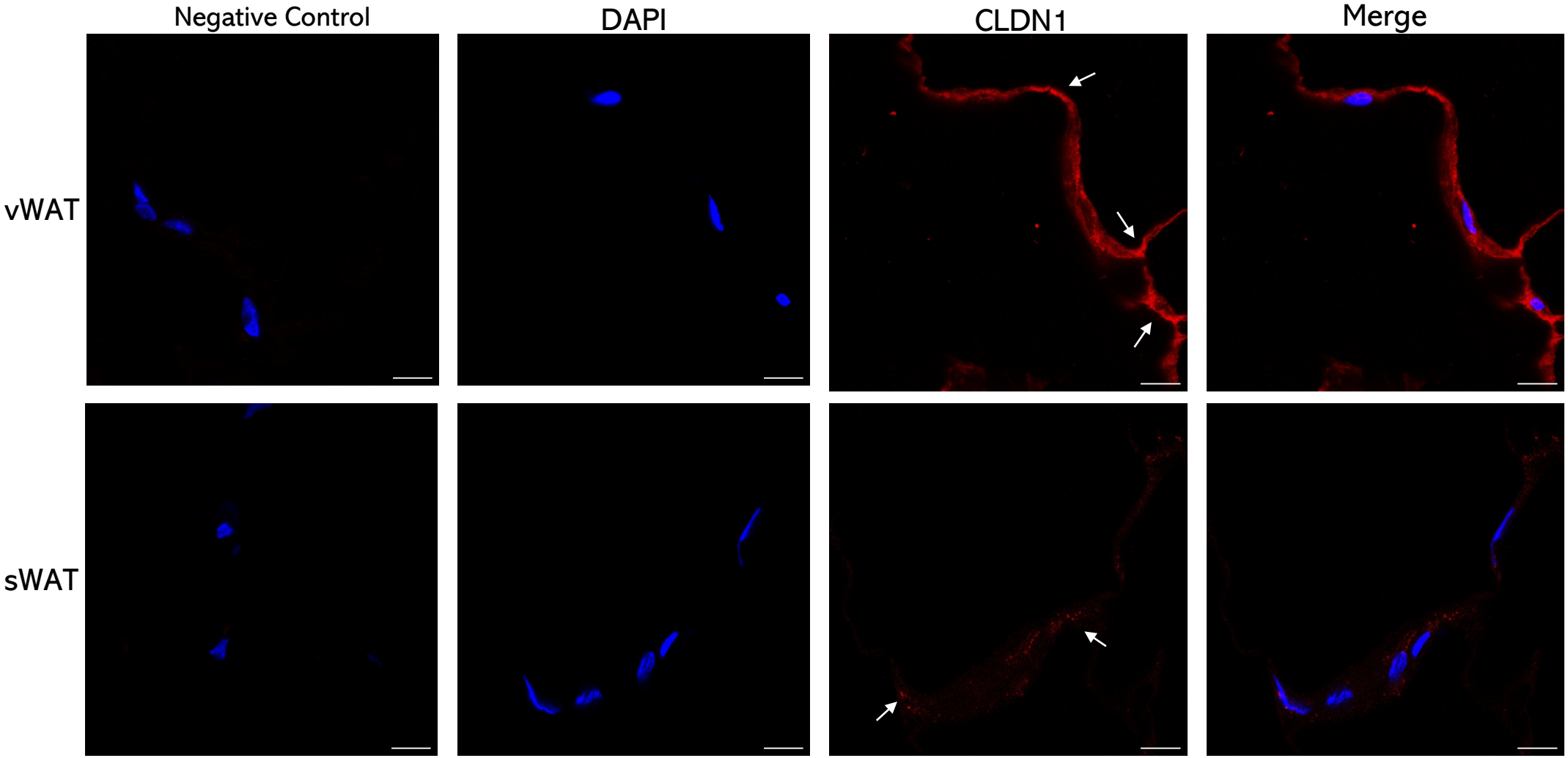
Negative Control
DAPI
CLDN1
Merge
vWAT
sWAT

**Table 1. Clinical parameters of Cohorts 1 and 2.** Cohort 1: 11 patients with severe obesity undergoing bariatric surgery (5 men and 6 women); Cohort 2: 14 controls and 13 patients with severe obesity undergoing bariatric surgery (all women). BMI: Body mass index; HbA1c: glycated hemoglobin, HOMA-IR: homeostatic model of insulin resistance; LDL-c: low-density lipoprotein cholesterol; HDL-c: high-density lipoprotein cholesterol. Differences between controls and patients with severe obesity were assessed using Student's t-test (normally-distributed) or Mann-Whitney test (nonnormally-distributed) for unpaired data. Normality was checked using the Shapiro–Wilk test. Statistical significance (Sig): * $p < 0.05$; ** $p < 0.01$; *** $p < 0.001$; **** $p < 0.0001$; ns—statistically not significant, controls vs patients with severe obesity (Cohort 2).

| | **Cohort 1** | **Cohort 2** | | |
|---|---|---|---|---|
| | **Obesity (*n*=11)** | **Control (*n*=14)** | **Obesity (*n*=13)** | **Sig.** |
| | **Mean ± SD** | **Mean ± SD** | **Mean ± SD** | |
| **Age (years)** | 50.9 ± 8.1 | 48.6 ± 8.2 | 46.2 ± 10.1 | ns |
| **Weight (kg)** | 113.5 ± 16.3 | 64.9 ± 9.40 | 112.2 ± 12.0 | **** |
| **BMI (kg/m$^2$)** | 40.6 ± 1.9 | 24.7 ± 2.5 | 43.5 ± 3.9 | **** |
| **Glucose (mg/dL)** | 117.6 ± 24.8 | 92.7 ± 15.4 | 106.5 ± 23.5 | ns |
| **Insulin ( mIU/L)** | 13.4 ± 11.3 | 5.4 ± 1.3 | 16.5 ± 11.8 | ns |
| **HbA1c (%)** | 5.5 ± 0.9 | 4.8 ± 0.8 | 5.3 ± 1.2 | ** |
| **HOMA-IR (%)** | 4.1 ± 4.40 | 1.3 ± 0.4 | 4.8 ± 4.2 | ns |
| **Triglycerides (mg/dL)** | 107 ± 39 | 72 ± 28 | 126 ± 34 | ** |
| **LDL-c (mg/dL)** | 110 ± 44 | 108 ± 31 | 91 ± 14 | ns |
| **HDL-c (mg/dL)** | 63 ± 42 | 68 ± 9 | 42 ± 8 | **** |
| **Total cholesterol (mg/dL)** | 187 ± 37 | 190 ± 34 | 158 ± 18 | * |

**Table 2:** Simple (Pearson's) correlation analyses for baseline *CLDN1* transcript expression levels in visceral (vWAT) and subcutaneous (sWAT) white adipose tissue and anthropometric and circulating variables in individuals from Cohort 2 at baseline (0M) and after 6 months of bariatric surgery (BS).

| | **0M** | | | | **6M** | | | |
|---|---|---|---|---|---|---|---|---|
| | **vWAT** | | **sWAT** | | **vWAT** | | **sWAT** | |
| | ***r*** | ***p*-value** | ***r*** | ***p*-value** | ***r*** | ***p*-value** | ***r*** | ***p*-value** |
| **Age** | 0.126 | 0.595 | 0.454 | 0.119 | NA | NA | NA | NA |
| **Surgery** | NA | NA | NA | NA | -0.145 | 0.636 | 0.671 | 0.144 |
| **Body weight** | 0.413 | 0.089 | 0.034 | 0.912 | -0.448 | 0.168 | 0.570 | 0.238 |
| **BMI** | 0.407 | 0.094 | -0.023 | 0.940 | -0.487 | 0.129 | **0.792** | ***0.048** |
| **Glucose** | 0.231 | 0.327 | 0.459 | 0.115 | -0.300 | 0.370 | 0.261 | 0.618 |
| **Insulin** | -0.057 | 0.853 | 0.090 | 0.817 | -0.313 | 0.413 | 0.520 | 0.370 |
| **HOMA1-IR** | -0.043 | 0.888 | 0.121 | 0.757 | -0.360 | 0.342 | 0.427 | 0.474 |
| **Hb1Ac** | **0.456** | ***0.043** | 0.152 | 0.745 | -0.193 | 0.592 | 0.130 | 0.806 |
| **cRP** | 0.609 | 0.109 | 0.608 | 0.584 | **0.791** | ***0.006** | **0.646** | ***0.044** |
| **TAG** | **0.521** | ***0.045** | -0.739 | 0.153 | -0.059 | 0.863 | 0.445 | 0.377 |
| **Total cholesterol** | -0.359 | 0.173 | 0.020 | 0.974 | 0.050 | 0.884 | 0.568 | 0.239 |
| **LDL-c** | -0.222 | 0.409 | 0.173 | 0.781 | 0.363 | 0.272 | 0.441 | 0.381 |
| **HDL-c** | **-0.587** | ***0.017** | -0.219 | 0.723 | -0.419 | 0.200 | 0.001 | 0.990 |

*N* = 20. BMI: Body Mass Index. HOMA1-IR: Homeostatic Model Assessment 1 for Insulin Resistance. TAG: Triacylglycerides. LDL-c: Low density lipoprotein cholesterol. HDL-c: High density lipoprotein cholesterol. Hb1Ac: glycated haemoglobin 1Ac. cRP: C-reactive protein. ρ: Spearman's rank correlation coefficient. *, bold: Statistically significant correlations ($p<0.05$).